

RAIST: Learning Risk Aware Traffic Interactions via Spatio-Temporal Graph Convolutional Networks

Videsh Suman, Phu Pham and Aniket Bera

Department of Computer Science, Purdue University, USA

Abstract—A key aspect of driving a road vehicle is to interact with other road users, assess their intentions and make risk-aware tactical decisions. An intuitive approach to enabling an intelligent automated driving system would be incorporating some aspects of human driving behavior. To this end, we propose a novel driving framework for egocentric views based on spatio-temporal traffic graphs. The traffic graphs not only model the spatial interactions amongst the road users, but also their individual intentions through temporally associated message passing. We leverage spatio-temporal graph convolutional network (ST-GCN) to train the graph edges. These edges are formulated using parameterized functions of 3D positions and scene-aware appearance features of road agents. Along with tactical behavior prediction, it is crucial to evaluate the risk-assessing ability of the proposed framework. We claim that our framework learns risk-aware representations by improving on the task of risk object identification, especially in identifying objects with vulnerable interactions like pedestrians and cyclists.

I. INTRODUCTION

Over the years, consistent research efforts toward autonomous driving led to significant developments in perception, planning, and control. A major challenge for autonomous vehicles is doing safe planning and driving decisions in urban traffic. In order to do so, we need to build robust methods for accurately and efficiently understanding traffic like human drivers and learn to analyze complex traffic scenes to make tactical driving decisions like slowing down, changing lanes, or taking turns. In moving traffic, making these decisions recklessly can cause road accidents and fatalities. To avoid such events, learning to identify potential risks in driving scenarios is critical. While visual cues are often the most useful source of perception and holistic scene understanding, utilizing this information to assess the behavior and interaction of individual road users is non-trivial. For urban driving scene understanding, we need to anticipate the behavior of dynamic and heterogeneous road agents in the traffic, including the vulnerable (pedestrians and cyclists) and other motorized not-so-vulnerable road agents, both spatially and temporally. Recent works [32], [57] have shown the promise of modeling spatial interactions amongst road users using interaction graphs. Interaction graphs are designed with the notion that every road user influences every other road user at a particular instant. However, current methods fail to model the behavior of individual road agents temporally. Anticipating the behavior of specific road agents is very crucial for humans to drive safely, and hence, this can be critical to autonomous vehicles for planning the navigation in impending traffic. For example, temporal intention modeling

can help the vehicle make critical distinctions between a scenario with a pedestrian waiting to cross and another with a pedestrian walking parallel to the road. Another example where temporal modeling can be helpful is to anticipate the intent of an approaching vehicle in a road intersection, i.e., in what direction will the vehicle continue moving?

Besides making the driving decisions, a better understanding of the scene, including road agents' intention modeling, can also be leveraged to assess the risk involved. Deep learning models are often uninterpretable, failing in surprising circumstances. An auxiliary goal of the risk assessment will increase the interpretability towards predicting driver-centric tactical behavior. The risk assessment literature [30] extensively covers the topic of potential risk identification. However, current methods like estimating object importance [21], [57] require carefully annotated training labels. Another plausible direction is to identify the *risk objects* that causally influence the ego-behavior [31]. While proposing a label-efficient causal inference method for identifying risk objects, it lacks interaction modeling and performs poorly, especially when the risk objects are pedestrians.

Main Contributions: We present a novel spatio-temporal learning framework for causal risk assessment from egocentric videos. We show that the proposed framework can generalize to multiple tasks that can benefit from interactive driving scene understanding. We use a combination of detection, tracking, depth estimation, and action recognition to obtain the attributes of road agents to formulate the edges of the spatio-temporal graphs. These spatio-temporal graphs are then used to compute a risk metric. The contributions are summarized below:

- We use the object attributes to model interaction edges amongst different object nodes at a particular instant. Each object node is also associated with its own representations across multiple time steps via temporal message passing. We parameterize the interaction edges and temporal message passing with respect to the vulnerability of the participating road agents.
- We use inpainting to remove the dynamic road agents from the input image frames followed by feature extraction in order to generate a frame-wise *static scene prior*. This scene prior is combined with each object's appearance features for context awareness, which is eventually used to model the graph edges.
- We evaluate this proposed approach on the task of risk object identification in a label-efficient manner using causal inference [31]. We detail the advantages of using

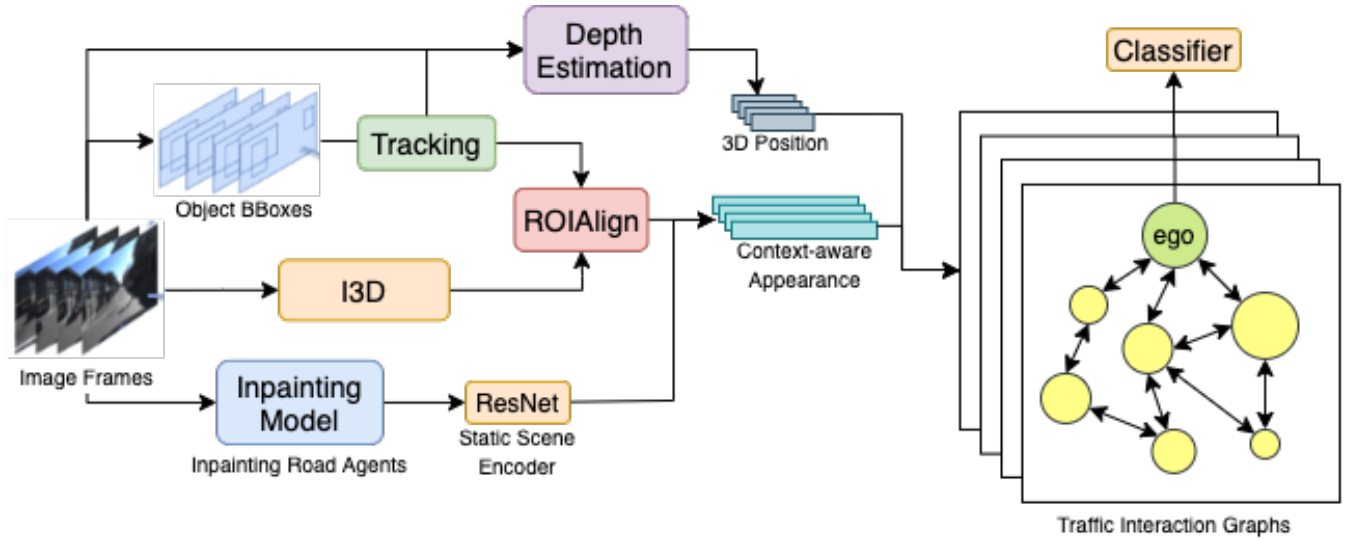


Fig. 1: An overview of the proposed driving model. The model takes a sequence of video frames as input, applies 3D convolutions (I3D backbone) to extract visual features, and employs ROIAlign to extract appearance features. Depth estimation and inpainting modules are used to obtain object-level 3D positions and inpainted frames with the background scenes, respectively. A static scene encoder is used to encode the inpainted images to obtain the context, which is further combined with the object-level appearance features. The modified features, along with the object-level 3D positions, are used to construct a frame-wise traffic interaction graph learned via spatio-temporal graph convolutional networks.

this framework to solve the causal problem in Section IV.

II. RELATED WORK

A. Driving Scene Understanding

There have been significant efforts in driver behavior understanding and tactical behavior recognition [37], [33], [29], [51]. In many classical approaches, hidden Markov models (HMM) were leveraged to recognize driver behaviors. A single node in HMM encodes the states from the ego vehicle, roads, and traffic participants into a state vector. In the proposed framework, we explicitly want to model two of these three states in the form of interactions between the ego and the other traffic agents. The third state of the roads is implicitly modeled using object-level context-aware features obtained from the static scene encoding. In the deep learning era, interesting methods like [40], [48], [32], [36] have been proposed to this end. Traffic trajectory prediction [9], [13], [14] and tracking [8], [12], [11], [10], have been widely studied in robotics and computer vision, whereas driver behavior modeling has mostly been restricted to traffic psychology and the social sciences [46], [22], [20], [19], [7], [25], [16], [17], [3], [1], [15], [2], [4], [35], [35], [34], [39], [43], [49].

B. Graph Convolutional Networks for Driving Scenes

Among other deep learning methods, graph convolutional networks [28] have made significant progress in tasks like action recognition [54], group activity recognition [52], scene graph generation [55], where the need is to learn the underlying semantic structure in the input videos.

For autonomous driving applications, very recent methods like [32], [36], [57] have been proposed that use graph convolutions to learn the spatial semantics of ego-centric driving scenarios. However, no work has focused on object-level temporal intention modeling using message passing via temporally associated nodes. We intend to use spatio-temporal GCNs [54] to achieve this.

C. Risk Assessment

It is natural for humans to assess risk before making decisions. This survey [30] presents some existing classical methods for motion prediction and risk assessment in the context of intelligent vehicles. It defines risk as the probability that the expectation and intention do not match any given traffic scenario. A similar definition of risk as being the object influencing the driver behavior was proposed in [31], and we intend to evaluate our framework's risk awareness using this definition. This task of risk object identification closely touches the boundaries of the task of object importance estimation [21], [57] where the goal is to detect semantically important objects in the ego-centric driving scenes. However, none of these past methods explicitly parameterize for the vulnerability [18] of the traffic participants with respect to the ego like we intend to do.

III. METHODOLOGY

This section describes our risk-aware driving scene understanding algorithm, the feature extraction pipeline, and the spatio-temporal graph-based approach.

A. Problem Statement

We propose a framework to predict tactical driver behavior and causal reasoning from driver-centric traffic for causal

risk assessment from egocentric videos. In this context, we define *tactical driver behavior* as the high-level driving decision resulting from a *cause* or the action of one or more participating dynamic road agents. For example, a tactical behavior can be *changing lane*, and the corresponding cause can be a *parked vehicle*. In practice, we tackle this as a classification problem with a fixed set of tactical behaviors and the corresponding cause.

Our framework exploits the underlying structure of a traffic scenario, including heterogeneity in traffic agents, by extracting the semantic features of traffic agents and using them to learn pair-wise spatial interactions that evolve temporally, hence learning a more generalizable and interpretable model.

B. Feature Extraction

Here we elaborate on the multiple feature extraction steps based on the semantics of the static and dynamic traffic scenarios.

Tracking and Location: With a sequence of Γ consecutive RGB frames $\mathcal{I}^{1:\Gamma}$, we use Faster R-CNN [42] to detect road agents in every frame. In order to identify each unique road agent across time, we then associate the obtained detections using Deep SORT [50]. This gives us N unique road agents, in terms of *tracklets*, where each tracklet \mathbf{r}_i stores the presence or absence of a road agent across the Γ time steps. Perspective projection makes it difficult to directly use the 2D pixel positions of objects to model spatial relations amongst them. To overcome this, we perform depth estimation [41] followed by inverse projection to transform every object's 2D pixel position to locate it in a 3D space with respect to the camera frame.

$$\begin{bmatrix} x & y & z \end{bmatrix}^T = \delta_{u,v} \mathbf{K}^{-1} \begin{bmatrix} u & v & 1 \end{bmatrix}^T \quad (1)$$

where (u, v) and (x, y, z) represents a point in 2D and 3D coordinate systems respectively. \mathbf{K} is the camera intrinsic matrix and $\delta_{u,v}$ is the relative depth at (u, v) obtained by depth estimation [41]. In the image plane, we select the center of a bounding box as that object's 2D position.

Appearance: To perform spatio-temporal reasoning on the road agents, we need rich features that are able to encode their inherent characteristics across all Γ time steps from the input $\mathcal{I}^{1:\Gamma}$. For this, we use Inception V1 [44] and I3D [5] as the global video descriptors and apply ROIAlign [23] over the 3D video feature map to obtain object-level appearance features from the corresponding regions of interest.

Static Scene Encoding: The appearance of road agents should also be associated with their static environment. To this end, we formulate a context extraction module in our framework. With $\mathcal{I}^{1:\Gamma}$ as the input, this module performs inpainting [56] to generate $\mathcal{S}^{1:\Gamma}$ image frames free from the dynamic agents of the scene. Following the inpainting, we use ResNet-18 [24] to encode $\mathcal{S}^{1:\Gamma}$ into frame-wise context embeddings $\mathbf{c}^{1:\Gamma}$. We update each object's appearance feature \mathbf{a}^t for time step t ,

$$\mathbf{a}^t \leftarrow \mathbf{a}^t \odot \mathbf{c}^t \quad (2)$$

Vulnerability: Vulnerable road agents are those that have little or no external protection and are at most risk in traffic [18]. In our design, we consider detected objects of classes *person, bicycle, car, motorcycle, bus, truck* as road agents, categorizing *person, bicycle* as **vulnerable** ($m = 1$) and the rest as non-vulnerable ($m = 0$). We use this categorization to learn a separate set of parameters for vulnerable road agents in the relation modeling.

In summary, we obtain N road agents and their frame-wise attributes from the input $\mathcal{I}^{1:\Gamma}$. For each road agent, we have (a) its tracklet \mathbf{r}_i , and if it exists in frame \mathcal{I}^t , we have its (b) category label m_i^t , (c) spatial position \mathbf{p}_i^t in 3D, and (d) scene-aware appearance feature \mathbf{a}_i^t . To perform spatio-temporal learning on graphs, we use the three mentioned attributes of road users.

C. Spatio-Temporal Modeling

The extracted features of road agents are used to create spatial interaction graphs with parameterized edges. We use spatio-temporal graph convolutions to learn the desired representations towards traffic scene understanding. We discuss this in detail here.

Graph Definition: In correspondence with $\mathcal{I}_{1:\Gamma}$, let $\mathbf{G}_{1:\Gamma}$ be the sequence of adjacency matrices, each of which can be realized as a graph with weighted edges between all existing nodes at that time step. Such a spatial graph \mathbf{G}_t can be interpreted as a traffic scene \mathcal{I}_t , where element $\mathbf{G}_t(i, j)$ denotes the influence of agent v_i^t over agent v_j^t . In any spatial graph \mathbf{G}_t , each node v_i^t can be represented as a tuple of its attributes $\{(\mathbf{a}_i^t, \mathbf{p}_i^t, m_i^t) | i = 1, 2, \dots, K+1\}$, assuming there are K road agents excluding the *ego*, a non-vulnerable road agent that is spatially located at the origin in the camera frame and whose context-aware appearance feature is based on the global output feature from the video encoder I3D.

Spatial Interaction Modeling: We believe that the interaction between any two road agents should be unique and depend on their respective attributes. To this end, we formulate the pair-wise spatial interactions using appearance and positional relations based on [52].

We represent the interaction value between nodes v_i^t and v_j^t with an entry in the adjacency matrix:

$$\mathbf{G}_t(i, j) = \frac{\mathbb{I}_d(\mathbf{p}_i^t, \mathbf{p}_j^t) f_p(\mathbf{p}_i^t, m_i^t, \mathbf{p}_j^t, m_j^t) \exp(f_a(\mathbf{a}_i^t, \mathbf{a}_j^t))}{\sum_{j=1}^{K+1} \mathbb{I}_d(\mathbf{p}_i^t, \mathbf{p}_j^t) f_p(\mathbf{p}_i^t, m_i^t, \mathbf{p}_j^t, m_j^t) \exp(f_a(\mathbf{a}_i^t, \mathbf{a}_j^t))} \quad (3)$$

where \mathbb{I}_d indicates the distance constraint, $f_p(\mathbf{p}_i^t, m_i^t, \mathbf{p}_j^t, m_j^t)$ indicates the vulnerability-dependent positional relation and $f_a(\mathbf{a}_i^t, \mathbf{a}_j^t)$ indicates the context-aware appearance relation. For every node, its edges are normalized, resembling a weighted softmax function. The influence of v_i^t over v_j^t is represented as a fraction of the total influence of v_i^t . The adjacency matrix \mathbf{G}_t also includes self-connections for self-attentional learning.

In order to restrict the interaction edges to objects that are spatially closer in traffic, we use the distance constraint as:

$$\mathbb{I}_d(\mathbf{p}_i^t, \mathbf{p}_j^t) = \mathbb{I}(d(\mathbf{p}_i^t, \mathbf{p}_j^t) \leq \mu) \quad (4)$$

where $\mathbb{I}(\cdot)$ is the indicator function, $d(\mathbf{p}_i^t, \mathbf{p}_j^t)$ is the Euclidean 3D distance between objects v_i^t and v_j^t , and μ is the distance threshold that constrains the interaction $\mathbf{G}_t(i, j)$ to be non-zero only if the spatial distance is lower than this upper bound. We use $\mu = 3$ in our framework.

The appearance relation is based on mutual similarity [47] and calculated as the scaled dot product between two embeddings as:

$$f_a(\mathbf{a}_i^t, \mathbf{a}_j^t) = \frac{\phi(\mathbf{a}_i^t)^T \omega(\mathbf{a}_j^t)}{\sqrt{D}} \quad (5)$$

where $\phi(\cdot)$ and $\omega(\cdot)$ are learnable linear transformations over the appearance features and D is the dimension of the embedding space. The parameters are learned to compute a scalar value for the influence of v_i^t over v_j^t in the embedding space. We note that this relation makes the overall spatial interaction directional, as $\phi(\cdot)$ and $\omega(\cdot)$ are different transformations.

For positional relation encoding, we use a vulnerability-dependent learnable transformation function $\theta_{m_i^t}(\mathbf{p}_i^t)$ to embed 3D positions. The pair-wise positional relation can be formulated as:

$$f_p(\mathbf{p}_i^t, m_i^t, \mathbf{p}_j^t, m_j^t) = \text{ReLU}\left(\mathbf{W}_p \gamma\left(\theta_{m_i^t}(\mathbf{p}_i^t) \odot \theta_{m_j^t}(\mathbf{p}_j^t)\right)\right) \quad (6)$$

where \odot denotes element-wise sum, and $\gamma(\cdot)$ is the Gaussian mapping function which encodes the embedded input into a high dimensional representation using sine and cosine of different wavelengths.

$$\gamma(\mathbf{v}) = [\cos(2\pi \mathbf{B}\mathbf{v}), \sin(2\pi \mathbf{B}\mathbf{v})]^T \quad (7)$$

where $\mathbf{v} \in \mathbb{R}^d$ is the input embedding vector and $\mathbf{B} \in \mathbb{R}^{k \times d}$ consists of entries sampled from $\mathcal{N}(0, \sigma^2)$, and σ is a hyperparameter. Here, $\gamma(\cdot)$ is used to embed d -dimensional input vector \mathbf{v} into $2k$ -dimensional vector. Such a Fourier feature mapping is effective in overcoming the spectral bias inherent in learning high-frequency functions in low dimensional domains [45] like the positional relation in our case. This mapping is then transformed into a scalar using trainable \mathbf{W}_p , followed by ReLU activation for non-linearity.

Spatio-Temporal Graph Reasoning: With the interaction graphs $\mathbf{G}_{1:\Gamma}$ formulated, we use spatio-temporal graph convolutional network (ST-GCN) [54] as the graph learning module over them. ST-GCN follows a similar implementation as GCN [28], which is followed by a convolution in the temporal domain. A layer of ST-GCN takes features as the input, leverages the spatial edges to aggregate the node-wise influence, and then uses spatial and temporal convolutional kernels to update the input features. For the purpose of simplification, we express l -th layer of ST-GCN at a particular time-step t ,

$$\mathbf{X}_t^{l'} = \text{ReLU}(\mathbf{G}_t \mathbf{X}_t^l \mathbf{W}_t^a) \quad (8)$$

$$\mathbf{X}_t^{l+1} = \text{ReLU}\left(\sum_{i=-\lfloor \tau/2 \rfloor}^{\lfloor \tau/2 \rfloor} \mathbf{X}_{t+i}^{l'} \mathbf{W}_{t+i}^b + \mathbf{X}_t^l\right) \quad (9)$$

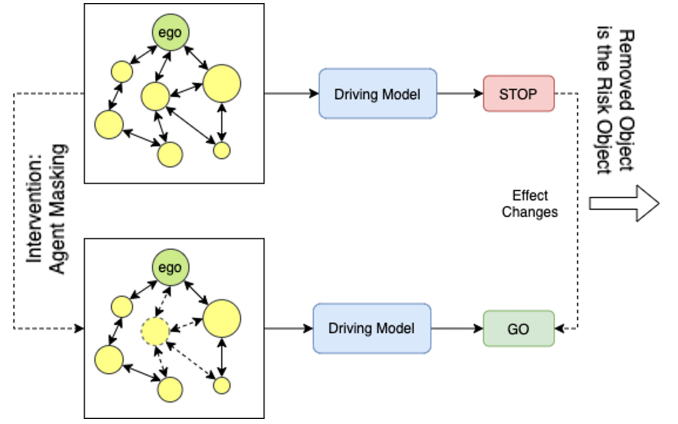


Fig. 2: Risk-identification using a two-step inference framework. In this scenario, intervening the input by removing the agent changes the driver's behavior (effect) from *Stop* to *Go*, indicating the omitted object is the risk object or the cause for *Stop*. In our framework, this intervention can be achieved by omitting the desired node from the traffic interaction graph.

where $\mathbf{G}_t \in \mathbb{R}^{N \times N}$ is the graph adjacency matrix, $\mathbf{X}_t^l \in \mathbb{R}^{N \times C}$ is l -th layer's feature map, ReLU is the activation function, $\mathbf{W}_t^a \in \mathbb{R}^{C \times C}$ and $\mathbf{W}_t^b \in \mathbb{R}^{C \times C}$ are the weight matrices for transformations in spatial and temporal dimensions respectively. In Equation (9), spatially attended interaction features are aggregated over τ consecutive time steps. There is a residual connection in each layer. In practice, this pair of transformations is implemented via 2D convolutional layers on a stack of frames in parallel, and the temporal span τ is used as the size of the temporally convolving kernel.

In the case of traffic scenarios, road agents keep varying across time. For effective temporal message passing, we need their associativity across Γ . In practice, the spatio-temporal adjacency matrix $\mathbf{G}_{1:\Gamma} \in \mathbb{R}^{\Gamma \times N \times N}$, and all the invalid interactions are zeroed based on the information from the tracklets $\mathbf{r}_{1:N}$. We use the context-aware appearance feature map stacked temporally as the input to the ST-GCN layers and update them after every layer. Following this, the interaction edges are remodeled with the updated features to be used for the next layer of ST-GCN. For learning the bias towards vulnerable road agents, we assign separate temporal convolutional weights to be shared across vulnerable and non-vulnerable agents.

IV. RISK ASSESSMENT

In this section, we discuss the task of risk object identification. Our proposed framework is designed to learn the spatio-temporal interactions in traffic, and we explain how it is an appropriate fit for this task.

A. Problem Statement

We use the driver-centric definition of risk to tackle the task of risk object identification or detecting the traffic agent that has the most significant influence over the ego's tactical behavior for a given scenario [31]. Due to the limited

annotations of real-world risk object bounding boxes, we choose to experiment with the cause-effect formulation of this task.

B. Causal Inference Setup

Given a traffic scenario $\mathcal{I}_{1:\Gamma}^{[1..N]}$ of Γ frames with N unique road agents, the proposed framework f is used to perform a two-stage inference:

- predict the high-level driving decision as *Stop* or *Go*

$$f : \mathcal{I}_{1:\Gamma}^{[1..N]} \rightarrow \{\text{Stop}, \text{Go}\} \quad (10)$$

- if the *Stop* prediction confidence is high,

$$Pr \left[f \left(\mathcal{I}_{1:\Gamma}^{[1..N]} \right) = \text{Stop} \right] \geq \delta \quad (11)$$

where δ is the thresholding hyperparameter, then the tracklet of risk object \mathbf{r}_o can be estimated by

$$o = \operatorname{argmax}_{i \in [1..N]} Pr \left[f \left(\mathcal{I}_{1:\Gamma}^{[1..N] \setminus i} \right) = \text{Go} \right] \quad (12)$$

where $\mathcal{I}_{1:\Gamma}^{[1..N] \setminus i}$ refers to the manipulated input by excluding tracklet \mathbf{r}_i from the original input $\mathcal{I}_{1:\Gamma}^{[1..N]}$, and $Pr \left[f \left(\mathcal{I}_{1:\Gamma}^{[1..N] \setminus i} \right) = \text{Go} \right]$ refers to the risk score s_i of agent with tracklet \mathbf{r}_i .

We note that this is a simplistic formulation to detect risk objects in critical *Stop* scenarios where some road agent might have a particularly high influence causing the ego's behavior to be *Stop*. The probability maximizing tracklet \mathbf{r}_o can be obtained from Equation (12) by performing iterative manipulations for each of the N road agents, one at a time. The risk evaluation is weakly supervised and only requires frame-level *Stop/Go* annotations for training.

C. Our Approach

The design of our proposed model allows for trivial manipulation of the traffic scenario with respect to each road agent by masking out its attributes before the graph modeling step. The spatio-temporal graph thus generated should closely represent an actual scenario without the particular agent. This avoids the artifacts that are introduced from masking directly in the input video frames [31]. We show improved results compared to the baseline in the next section.

We realize a drawback in the above causal inference setup towards safe risk assessment. Let's consider a scenario with multiple pedestrians crossing in front of the ego, and the original tactical behavior is correctly classified as *Stop*. In such a case, unless the crossing pedestrians are removed all at once, the driving model's prediction shouldn't change from *Stop* to *Go*, i.e., any pedestrian's individual risk score s_i needn't be very high. Hence, we can cherry-pick such scenarios from the dataset and identify the corresponding *risk groups* based on their high interaction values with respect to the ego node in the spatio-temporal graph $\mathbf{G}_{1:\Gamma}$. For some of these scenarios, we perform the causal inference step with a single manipulation for the entire risk group and show the risk scores in this visualization.

V. EXPERIMENTS

A. Dataset

For the tactical behavior prediction task, we evaluate on the HDD dataset [40]. It is a challenging dataset that facilitates research in learning driver behavior in real-life settings. The dataset comprises 104 hours of actual human driving in the San Francisco Bay Area, captured using a vehicle fitted with various sensors. The authors showcase instances of goal-driven driving behavior from the dataset in the videos provided, which include GPS coordinates and CAN bus sensor data overlaid on the front-facing camera stream. The dataset provides driver-centric videos with frame-level annotations of tactical driver behavior and the associated cause. The dataset consists of diverse road scenarios, including urban, suburban, and highways.

Each frame is labeled by a 4-layer representation to describe the tactical driver behaviors. Among these 4 layers, **Goal-oriented** action layer (e.g., left turn and right lane change) and **Cause** layer (e.g., stop for crossing vehicle) consist of the actions with interactions. We leverage the labels from these two layers to analyze the effectiveness of the proposed interaction modeling framework.

For the causal risk object identification task, we use the same dataset, leveraging the layers of **Stimulus-driven action** with labels of *Stop* and *deviate*, and **cause** denoting the reason for the associated stimulus-driven behavior. In total, the dataset has scenarios labeled with six types of **Cause**, i.e., *Stopping for Congestion*, *Stopping for Crossing Vehicle*, *Deviating for Parked Vehicle*, *Stopping for Pedestrian*, *Stopping for Sign*, and *Stopping for Red Light*. The first four scenarios are selected to evaluate the proposed risk object identification framework since our proposed framework is based on the interactions between the dynamic road agents only. We intend to utilize the frame-level driver behavior labels (i.e., *Go* and *Stop*) to train our driving model for risk assessment. For evaluating the task of risk identification, we use the object-level annotations [31] provided.

B. Evaluation metrics

We evaluate the performance of our model using mean accuracy ($mAcc$). Accuracy is computed as the number of correct predictions over the number of ground truth samples. A prediction is considered accurate if the Intersection over Union (IoU) score is greater than a certain threshold. We compute $mAcc$ as the average accuracy at 10 IoU thresholds, uniformly distributed in the range of 0.5 – 0.95.

C. Implementation Details

For tactical behavior prediction, we use 20-frame clips with resolution 200×356 at 3 fps as the input to the framework. We use the I3D network [6] pre-trained on the Kinetics action recognition dataset [26] as the backbone for encoding the global video features. The intermediate video feature map from the `Mixed_3c` layer of I3D is used in the `ROIAlign` layer to obtain the appearance features. In our implementation, we use the appearance embedding dimension $D = 256$. For encoding the positional relations

Method	<i>mAcc (%)</i>			
	Crossing Vehicle	Crossing Pedestrian	Parked Vehicle	Congestion
Random Selection	15.1	7.1	6.4	5.5
Driver’s Attention Prediction * [53]	16.8	8.9	10.0	21.3
Object-level Attention Selector [48]	36.5	21.2	20.1	8.9
Pixel-level Attention + Causality Test [27]	41.9	21.5	34.6	62.7
Who Make Drivers Stop? [31]	43.0	27.0	39.8	81.0
Ours	42.7	28.6	41.3	87.9

TABLE I: Comparison with baseline methods. The methods with * are reimplemented by Li et al. [31]. The best and second performances are colored in red and orange, respectively.

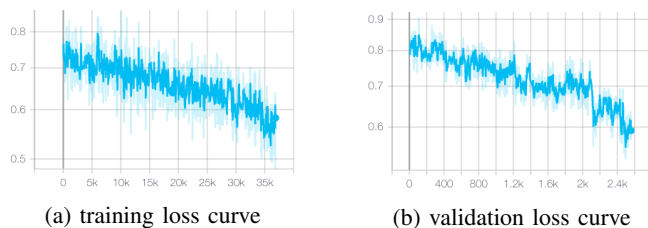


Fig. 3: We present the training and validation loss curves obtained from the training for 40 epochs.

using $\gamma(\cdot)$, we choose $d = 5$, $k = 30$ and follow [45] to choose $\sigma = 10$. We stack three layers of ST-GCN, i.e., the pair of equations (8) and (9) with temporal span $\tau = 3$. The last layer of ST-GCN is followed by the classifier that includes average pooling and fully connected layers to obtain the classification logits, which are further converted into class probabilities using the softmax layer. Each layer of a neural network is followed by a layer of batch normalization. We use Adam as the optimizer with default parameters and an initial learning rate of 0.001. We are implementing the framework on PyTorch [38] and performing all experiments on a node with 4 Nvidia Tesla M40 GPUs.

VI. QUANTITATIVE EVALUATION

Risk object identification is a relatively new area of research in the autonomous driving community. We compare with previous approaches in this area to select important/risk objects. The comparison with our method is shown in TABLE I. We represent the performance of our approach on top of the results of several baseline methods reported in [31].

Random Selection: This baseline method identifies a risk object by randomly selecting an object detected in a frame without considering any surrounding information. The Driver’s Attention Prediction method uses a pre-trained model [53] to predict the driver’s gaze attention maps for each frame. The method calculates the average attention weight of each detected object region and designates the object with the highest attention weight as the risk object, indicating where the driver’s gaze is focused. The model is trained from a pre-trained model of the BDD-A dataset [53] since the HDD dataset lacks human gaze information. Compared to Random Selection, this method delivers slightly superior performance.

Pixel-level Attention + Causality Test: Kim et al. [27] devised a causality test for identifying regions that influence a network’s output. To achieve this, they created a pixel-level attention map using an end-to-end driving model to extract particles based on attention value over an input image. These particles were then clustered to create convex hull region proposals. An RGB image was evaluated repeatedly by the trained model to conduct a causality test, and the region that resulted in the largest decrease in prediction performance was deemed the risk object.

Object-level Attention Selector: Wang et al. [48] developed a driving model that concentrates on objects by learning attention weights at the object level, enabling the identification of risky objects. We were influenced by their methodology and modified the message passing in our driving model to integrate object-level attention, following which we retrained the model. Subsequently, we evaluated the model’s accuracy by selecting the object with the highest attention weight in four distinct scenarios.

Who Make Drivers Stop?: Li et al. [31] suggests a new definition of risk that focuses on objects that impact a driver’s behavior. Motivated by design by Wang et al. [48], the authors modify the message passing in the driving model to be object-level attention and retrain their model. They propose a new task called risk object identification, which aims to solve a cause-effect problem. The authors introduce a two-stage risk object identification framework that relies on causal inference and the object-level manipulable driving model.

We compare the performance of these models with our approach. As indicated in Table I, Random Selection and Driver’s Attention Prediction models are inferior in comparison to other models. The Object-level Attention Selector approach achieves better results but performs poorly on congestion tasks. Pixel-level Attention and Causality Test achieve better performance, but still worse than Who Make Drivers Stop in all the tasks. Our model achieves top results in 3 out of 4 tasks. For the crossing vehicle setting, our result is very close to that of the top model.

VII. CONCLUSION, LIMITATIONS, AND FUTURE WORK

We propose a novel framework for autonomous driving that models spatio-temporal traffic graphs to incorporate aspects of human driving behavior. The framework utilizes spatio-temporal graph convolutional networks to train graph

edges, which are formulated using parameterized functions of 3D positions and scene-aware appearance features of road agents. The proposed framework can learn risk-aware representations by improving the task of identifying objects with vulnerable interactions, such as pedestrians and cyclists. The experimental results show that our approach outperforms all other baseline models in most tasks.

In the future, we plan to analyze our network and integrate psychology-derived traffic interaction algorithms into our model. There are several potential avenues for future research in the area of driver risk prediction. One important direction is to explore the use of multimodal data sources, such as incorporating information from vehicle sensors, driver biometric sensors, and external environment sensors, to improve the accuracy of risk prediction. Another area of research could focus on developing more sophisticated models that incorporate deep learning and reinforcement learning techniques to better capture the complex relationships between driving behaviors and risk factors. Additionally, evaluating the performance of driver risk prediction models in real-world scenarios is necessary to assess their practical usefulness and identify any limitations. Finally, the development of explainable AI techniques could be beneficial in increasing the interpretability and transparency of driver risk prediction models, promoting their wider adoption and trust among stakeholders such as drivers, insurers, and regulators.

REFERENCES

- [1] Ahmad Aljaafreh, Nabeel Alshabat, and Munaf S. Najim Al-Din. Driving style recognition using fuzzy logic. *2012 IEEE International Conference on Vehicular Electronics and Safety (ICVES 2012)*, pages 460–463, 2012.
- [2] Kenneth H. Beck, Bina Ali, and Stacey B Daughters. Distress tolerance as a predictor of risky and aggressive driving. *Traffic injury prevention*, 15 4:349–54, 2014.
- [3] Aniket Bera, Tanmay Randhavan, and Dinesh Manocha. Aggressive, tense or shy? identifying personality traits from crowd videos. In *IJCAI*, 2017.
- [4] J Christopher Brill, Mustapha Mouloua, Edwin Shirkey, and Pascal Alberti. Predictive validity of the aggressive driver behavior questionnaire (adbq) in a simulated environment. In *Proceedings of the Human Factors and Ergonomics Society Annual Meeting*, volume 53, pages 1334–1337. SAGE Publications Sage CA: Los Angeles, CA, 2009.
- [5] Joao Carreira and Andrew Zisserman. Quo vadis, action recognition? a new model and the kinetics dataset. In *Proceedings of the IEEE Conference on Computer Vision and Pattern Recognition (CVPR)*, July 2017.
- [6] Joao Carreira and Andrew Zisserman. Quo vadis, action recognition? a new model and the kinetics dataset. In *proceedings of the IEEE Conference on Computer Vision and Pattern Recognition*, pages 6299–6308, 2017.
- [7] Rohan Chandra, Aniket Bera, and Dinesh Manocha. Stylepredict: Machine theory of mind for human driver behavior from trajectories. *arXiv preprint arXiv:2011.04816*, 2020.
- [8] Rohan Chandra, Uttaran Bhattacharya, Aniket Bera, and Dinesh Manocha. Densepeds: Pedestrian tracking in dense crowds using front-view and sparse features. *arXiv preprint arXiv:1906.10313*, 2019.
- [9] Rohan Chandra, Uttaran Bhattacharya, Aniket Bera, and Dinesh Manocha. Traffic: Trajectory prediction in dense and heterogeneous traffic using weighted interactions. In *Proceedings of the IEEE Conference on Computer Vision and Pattern Recognition*, pages 8483–8492, 2019.
- [10] Rohan Chandra, Uttaran Bhattacharya, Trisha Mittal, Aniket Bera, and Dinesh Manocha. Cmetric: A driving behavior measure using centrality functions. *arXiv preprint arXiv:2003.04424*, 2020.
- [11] Rohan Chandra, Uttaran Bhattacharya, Trisha Mittal, Xiaoyu Li, Aniket Bera, and Dinesh Manocha. Graphrqi: Classifying driver behaviors using graph spectrums. *arXiv preprint arXiv:1910.00049*, 2019.
- [12] Rohan Chandra, Uttaran Bhattacharya, Tanmay Randhavan, Aniket Bera, and Dinesh Manocha. Roadtrack: Realtime tracking of road agents in dense and heterogeneous environments. *arXiv*, pages arXiv–1906, 2019.
- [13] Rohan Chandra, Uttaran Bhattacharya, Christian Roncal, Aniket Bera, and Dinesh Manocha. Robusttp: End-to-end trajectory prediction for heterogeneous road-agents in dense traffic with noisy sensor inputs. In *ACM Computer Science in Cars Symposium*, pages 1–9, 2019.
- [14] Rohan Chandra, Tianrui Guan, Srujan Panuganti, Trisha Mittal, Uttaran Bhattacharya, Aniket Bera, and Dinesh Manocha. Forecasting trajectory and behavior of road-agents using spectral clustering in graph-lstms. *IEEE Robotics and Automation Letters*, 2020.
- [15] Ernest Cheung, Aniket Bera, Emily Kubin, Kurt Gray, and Dinesh Manocha. Classifying driver behaviors for autonomous vehicle navigation. 2018.
- [16] Ernest Cheung, Aniket Bera, Emily Kubin, Kurt Gray, and Dinesh Manocha. Identifying driver behaviors using trajectory features for vehicle navigation. In *2018 IEEE/RSJ International Conference on Intelligent Robots and Systems (IROS)*, pages 3445–3452. IEEE, 2018.
- [17] Ernest Cheung, Aniket Bera, and Dinesh Manocha. Efficient and safe vehicle navigation based on driver behavior classification. In *Proceedings of the IEEE Conference on Computer Vision and Pattern Recognition Workshops*, pages 1024–1031, 2018.
- [18] Aymery Constant and Emmanuel Lagarde. Protecting vulnerable road users from injury. *PLoS Med*, 7(3):e1000228, 2010.
- [19] Jerry L Deffenbacher, Eugene R Oetting, and Rebekah S Lynch. Development of a driving anger scale. *Psychological reports*, 1994.
- [20] Davina J French, Robert J West, James Elander, and John Martin WILDING. Decision-making style, driving style, and self-reported involvement in road traffic accidents. *Ergonomics*, 36(6):627–644, 1993.
- [21] Mingfei Gao, Ashish Tawari, and Sujitha Martin. Goal-oriented object importance estimation in on-road driving videos. In *2019 International Conference on Robotics and Automation (ICRA)*, pages 5509–5515. IEEE, 2019.
- [22] E Gulian, G Matthews, Aleck Ian Glendon, DR Davies, and LM Debney. Dimensions of driver stress. *Ergonomics*, 1989.
- [23] Kaiming He, Georgia Gkioxari, Piotr Dollár, and Ross Girshick. Mask r-cnn. In *Proceedings of the IEEE international conference on computer vision*, pages 2961–2969, 2017.
- [24] Kaiming He, Xiangyu Zhang, Shaoqing Ren, and Jian Sun. Deep residual learning for image recognition. In *Proceedings of the IEEE conference on computer vision and pattern recognition*, pages 770–778, 2016.
- [25] Motonori Ishibashi, Masayuki Okuwa, Shun’ichi Doi, and Motoyuki Akamatsu. Indices for characterizing driving style and their relevance to car following behavior. In *SICE Annual Conference 2007*, pages 1132–1137. IEEE, 2007.
- [26] Will Kay, Joao Carreira, Karen Simonyan, Brian Zhang, Chloe Hillier, Sudheendra Vijayanarasimhan, Fabio Viola, Tim Green, Trevor Back, Paul Natsev, et al. The kinetics human action video dataset. *arXiv preprint arXiv:1705.06950*, 2017.
- [27] Jinkyu Kim and John Canny. Interpretable learning for self-driving cars by visualizing causal attention. In *Proceedings of the IEEE international conference on computer vision*, pages 2942–2950, 2017.
- [28] Thomas N Kipf and Max Welling. Semi-supervised classification with graph convolutional networks. *arXiv preprint arXiv:1609.02907*, 2016.
- [29] Nobuyuki Kuge, Tomohiro Yamamura, Osamu Shimoyama, and Andrew Liu. A driver behavior recognition method based on a driver model framework. *SAE transactions*, pages 469–476, 2000.
- [30] Stéphanie Lefèvre, Dizan Vasquez, and Christian Laugier. A survey on motion prediction and risk assessment for intelligent vehicles. *ROBOMECH journal*, 1(1):1–14, 2014.
- [31] Chengxi Li, Stanley H Chan, and Yi-Ting Chen. Who make drivers stop? towards driver-centric risk assessment: Risk object identification via causal inference. *arXiv preprint arXiv:2003.02425*, 2020.
- [32] Chengxi Li, Yue Meng, Stanley H Chan, and Yi-Ting Chen. Learning 3d-aware egocentric spatial-temporal interaction via graph convolutional networks. In *2020 IEEE International Conference on Robotics and Automation (ICRA)*, pages 8418–8424. IEEE, 2020.
- [33] Dejan Mitrovic. Reliable method for driving events recognition. *IEEE transactions on intelligent transportation systems*, 6(2):198–205, 2005.
- [34] Ishak Mohamad, Mohd. Alauddin Mohd. Ali, and Mahamod Ismail. Abnormal driving detection using real time global positioning system data. *Proceeding of the 2011 IEEE International Conference on Space Science and Communication (IconSpace)*, pages 1–6, 2011.

- [35] Yi Lu Murphey, Richard Milton, and Leonidas Kiliaris. Driver's style classification using jerk analysis. *2009 IEEE Workshop on Computational Intelligence in Vehicles and Vehicular Systems*, pages 23–28, 2009.
- [36] Sravan Mylavarapu, Mahtab Sandhu, Priyesh Vijayan, K Madhava Krishna, Balaraman Ravindran, and Anoop Namboodiri. Understanding dynamic scenes using graph convolution networks. *arXiv preprint arXiv:2005.04437*, 2020.
- [37] Nuria Oliver and Alex P Pentland. Graphical models for driver behavior recognition in a smartcar. In *Proceedings of the IEEE Intelligent Vehicles Symposium 2000 (Cat. No. 00TH8511)*, pages 7–12. IEEE, 2000.
- [38] Adam Paszke, Sam Gross, Francisco Massa, Adam Lerer, James Bradbury, Gregory Chanan, Trevor Killeen, Zeming Lin, Natalia Gimelshein, Luca Antiga, et al. Pytorch: An imperative style, high-performance deep learning library. In *Advances in neural information processing systems*, pages 8026–8037, 2019.
- [39] Geqi Qi, Yiman Du, Jianping Wu, and Ming Xu. Leveraging longitudinal driving behaviour data with data mining techniques for driving style analysis. *IET intelligent transport systems*, 9(8):792–801, 2015.
- [40] Vasili Ramanishka, Yi-Ting Chen, Teruhisa Misu, and Kate Saenko. Toward driving scene understanding: A dataset for learning driver behavior and causal reasoning. In *Proceedings of the IEEE Conference on Computer Vision and Pattern Recognition*, pages 7699–7707, 2018.
- [41] R. Ranftl, K. Lasinger, D. Hafner, K. Schindler, and V. Koltun. Towards robust monocular depth estimation: Mixing datasets for zero-shot cross-dataset transfer. *IEEE Transactions on Pattern Analysis and Machine Intelligence*, pages 1–1, 2020.
- [42] Shaoqing Ren, Kaiming He, Ross Girshick, and Jian Sun. Faster r-cnn: Towards real-time object detection with region proposal networks. In *Advances in neural information processing systems*, pages 91–99, 2015.
- [43] Bin Shi, Li Xu, Jie Hu, Yun Tang, Hong Jiang, Wuqiang Meng, and Hui Liu. Evaluating driving styles by normalizing driving behavior based on personalized driver modeling. *IEEE Transactions on Systems, Man, and Cybernetics: Systems*, 45:1502–1508, 2015.
- [44] Christian Szegedy, Wei Liu, Yangqing Jia, Pierre Sermanet, Scott Reed, Dragomir Anguelov, Dumitru Erhan, Vincent Vanhoucke, and Andrew Rabinovich. Going deeper with convolutions. In *Proceedings of the IEEE conference on computer vision and pattern recognition*, pages 1–9, 2015.
- [45] Matthew Tancik, Pratul P Srinivasan, Ben Mildenhall, Sara Fridovich-Keil, Nithin Raghavan, Utkarsh Singhal, Ravi Ramamoorthi, Jonathan T Barron, and Ren Ng. Fourier features let networks learn high frequency functions in low dimensional domains. *arXiv preprint arXiv:2006.10739*, 2020.
- [46] Orit Taubman-Ben-Ari, Mario Mikulincer, and Omri Gillath. The multidimensional driving style inventory—scale construct and validation. *Accident Analysis & Prevention*, 36(3):323–332, 2004.
- [47] Ashish Vaswani, Noam Shazeer, Niki Parmar, Jakob Uszkoreit, Llion Jones, Aidan N Gomez, Łukasz Kaiser, and Illia Polosukhin. Attention is all you need. In *Advances in neural information processing systems*, pages 5998–6008, 2017.
- [48] Dequan Wang, Coline Devin, Qi-Zhi Cai, Fisher Yu, and Trevor Darrell. Deep object-centric policies for autonomous driving. In *2019 International Conference on Robotics and Automation (ICRA)*, pages 8853–8859. IEEE, 2019.
- [49] Wenshuo Wang, Junqiang Xi, Alexandre Chong, and Lin Li. Driving style classification using a semisupervised support vector machine. *IEEE Transactions on Human-Machine Systems*, 47:650–660, 2017.
- [50] Nicolai Wojke, Alex Bewley, and Dietrich Paulus. Simple online and realtime tracking with a deep association metric. In *2017 IEEE international conference on image processing (ICIP)*, pages 3645–3649. IEEE, 2017.
- [51] Bing-Fei Wu, Ying-Han Chen, Chung-Hsuan Yeh, and Yen-Feng Li. Reasoning-based framework for driving safety monitoring using driving event recognition. *IEEE Transactions on Intelligent Transportation Systems*, 14(3):1231–1241, 2013.
- [52] Jianchao Wu, Limin Wang, Li Wang, Jie Guo, and Gangshan Wu. Learning actor relation graphs for group activity recognition. In *Proceedings of the IEEE Conference on Computer Vision and Pattern Recognition*, pages 9964–9974, 2019.
- [53] Ye Xia, Danqing Zhang, Jinkyu Kim, Ken Nakayama, Karl Zipser, and David Whitney. Predicting driver attention in critical situations. In C.V. Jawahar, Hongdong Li, Greg Mori, and Konrad Schindler, editors, *Computer Vision – ACCV 2018*, pages 658–674, Cham, 2019. Springer International Publishing.
- [54] Sijie Yan, Yuanjun Xiong, and Dahua Lin. Spatial temporal graph convolutional networks for skeleton-based action recognition. *arXiv preprint arXiv:1801.07455*, 2018.
- [55] Jianwei Yang, Jiasen Lu, Stefan Lee, Dhruv Batra, and Devi Parikh. Graph r-cnn for scene graph generation. In *Proceedings of the European conference on computer vision (ECCV)*, pages 670–685, 2018.
- [56] Jiahui Yu, Zhe Lin, Jimei Yang, Xiaohui Shen, Xin Lu, and Thomas S Huang. Generative image inpainting with contextual attention. In *Proceedings of the IEEE conference on computer vision and pattern recognition*, pages 5505–5514, 2018.
- [57] Zehua Zhang, Ashish Tawari, Sujitha Martin, and David Crandall. Interaction graphs for object importance estimation in on-road driving videos. *arXiv preprint arXiv:2003.06045*, 2020.